Magnetic Carbon Nanotubes: Synthesis by Electrostatic Self-Assembly Approach and Application in Biomanipulations

ARTICLE *in* THE JOURNAL OF PHYSICAL CHEMISTRY B · MAY 2006

Impact Factor: 3.3 · DOI: 10.1021/jp0602474 · Source: PubMed

5 AUTHORS, INCLUDING:

Chao Gao
Zhejiang University
138 PUBLICATIONS **7,566** CITATIONS

SEE PROFILE

Magnetic Carbon Nanotubes: Synthesis by Electrostatic Self-Assembly Approach and Application in Biomanipulations

Chao Gao,*,† Wenwen Li,† Hisao Morimoto,‡ Yutaka Nagaoka,‡ and Toru Maekawa*,‡

College of Chemistry and Chemical Engineering, Shanghai Jiao Tong University, 800 Dongchuan Road, Shanghai 200240, P. R. China and Bio-Nano Electronics Research Centre, Toyo University, 2100, Kujirai, Kawagoe, Saitama 350-8585, Japan

Received: January 13, 2006; In Final Form: February 20, 2006

Magnetic multiwalled carbon nanotubes (MWNTs) were facilely prepared by the electrostatic self-assembly approach. Poly(2-diethylaminoethyl methacrylate) (PDEAEMA) was covalently grafted onto the surfaces of MWNTs by MWNT-initiated in situ atom transfer radical polymerization (ATRP) of 2-diethylaminoethyl methacrylate (DEAEMA). The PDEAEMA-grafted MWNTs were quaternized with methyl iodide (CH_3I), resulting in cationic polyelectrolyte-grafted MWNTs (MWNT-PAmI). Magnetic iron oxide (Fe_3O_4) nanoparticles were loaded onto the MWNT surfaces by electrostatic self-assembling between MWNT-PAmI and Fe_3O_4, affording magnetic nanotubes. The assembled capability of the nanoparticles can be adjusted to some extent by changing the feed ratio of Fe_3O_4 to MWNT-PAmI. The obtained magnetic nanotubes were characterized with TEM, EDS, STEM, and element mapping analyses. TEM and EDS measurements confirmed the nanostructures and the components of the resulting nanoobjects. The magnetic nanotubes were assembled onto sheep red blood cells in a phosphate buffer solution, forming magnetic cells. The blood cells attached with or without magnetic nanotubes can be selectively manipulated in a magnetic field. These results promise a general and efficient strategy to magnetic nanotubes and the fascinating potential of such magnetic nanoobjects in applications of bionanoscience and technology.

1. Introduction

Carbon nanotubes (CNTs)[1] have become one of the most commonly mentioned constructive nanomaterials and building blocks of nanotechnology since their discovery in 1991 due to their unique electronic, mechanical, and chemical properties and their fascinating one-dimensional (1D) tubular structures.[2] Depending on the connatural properties such as high modulus and high electrical and thermal conductivities and the ability to carry high currents, etc., CNTs can be used to fabricate numerous novel nanocomposites and nanodevices. By employing their tubular hollow cavity, CNTs can be utilized as containers and reactors to prepare nanodevices and nanostructures such as nanothermometer[3] and peapods.[4] Except these, the convex surface of CNTs is also a tremendous resource which is very useful to transfer mass or ions and support guest compounds as a substrate.[5,6] In this regard, organic small molecules,[7] complexes,[8] surfactants,[9] macromolecules,[10] metals,[11] oxides,[12] and quantum dots (QDs)[13] could be attached or coated onto convex surfaces of CNTs by covalent linkage, physical adsorption, chemical vapor deposition (CVD), and other methods and techniques. Thus, a plentiful appearance of functional hybrid nanomaterials, nanodevices, and nanostructures are expected by means of designing and tailoring.

The main purposes of this work are to present a facile, a general, and an effective approach to magnetic nanotubes based on the convex surfaces of CNTs and then to explore the potential application of the as-prepared magnetic nanotubes as a magnetic handle for biomanipulations. Recently, paramagnetic nanotubes have been prepared by filling CNTs with iron oxide particles.[14] Although the possibly loaded capacity of magnetic particles is very high, the drawbacks of such strategy are obvious: (1) the source of CNTs is not general because the employed CNTs are required to prepare with a specific method of alumina template; (2) the used tubes are very big (the average outer diameter is ca. 300 nm), which means that the product is not a real "nano", object and thus its application is limited in the actual "nano" realm (1−100 nm); (3) such strategy cannot be extended to the conventional CNTs because they generally contain many inside knars, especially for CVD tubes, and their ends are closed. Since the strategy of filling CNTs inside is not so common, the strategy of attaching magnetic particles onto CNTs outside is an alternate choice. Georgakilas et al. attached pyrene-linked iron oxide nanoparticles onto single-walled carbon nanotubes (SWNTs) to prepare magnetic nanotubes based on the $\pi-\pi$ stacking interactions between CNTs and pyrene moiety.[15] The disadvantages of such method lie in the following: (1) the attachment is very weak because the attaching force of $\pi-\pi$ stacking interaction is not strong itself and now gets weaker due to the weighing of iron oxide particles; (2) the loading capability of magnetic particles is quite low because of such weak attaching, which limits the applications of the product; (3) the attaching effectivity would be much lower if it is extended to multiwalled carbon nanotubes (MWNTs) because the surface area per gram of MWNTs is much smaller than that of SWNTs. Herein, we present a general approach to magnetic nanotubes which overcomes the shortcomings aforementioned. In addition, the application of the as-prepared magnetic nanotubes in the biomanipulations is being explored.

* To whom correspondence should be addressed. Phone: +86-21-54742665. Fax: +86-21-54741297. E-mail: chaogao@sjtu.edu.cn (C.G.), trmkw@eng.toyo.ac.jp (T.M.).

† Shanghai Jiao Tong University.

‡ Toyo University.

10.1021/jp0602474 CCC: $33.50
Published on Web 03/17/2006

2. Experimental Section

Materials. Pristine MWNTs made by the CVD method were purchased from Tsinghua-Nafine Nano-Powder Commercialization Engineering Centre in Beijing (purity > 95%). MWNT-based macroinitiator (MWNT-Br) was synthesized according to a previous paper.[16] Monomer, 2-diethylaminoethyl methacrylate (DEAEMA), was purchased from Aldrich. The inhibitor was removed by passage through an alumina column, followed by vacuum distillation. CuBr (Aldrich) was purified by extraction with glacial acetic acid overnight and then washed with alcohol and ether. Methyl iodide (CH_3I) and *N*,*N*,*N*′,*N*″,*N*″-pentmethyldiethylenetriamine (PMDETA) were purchased from Acros and used as received. Sheep blood was purchased from Nippon Bio-Supp. Center. Sheep's erythrocytes, which were separated from the blood using a centrifuge (CN-2060, Hsiangtai Machinery Ind. Co. Ltd.), were dispersed in phosphate-buffered saline (PBS) solution (pH 7.4) for the manipulation experiment. Magnetic nanoparticles (Taiho Industry Co. Ltd.), which are made of magnetite (Fe_3O_4), were dispersed in water. The surface of each particle is coated with anionic surfactant for the stable dispersion.

Instrumentation. Fourier transform infrared (FTIR) spectra were recorded on a PE Paragon 1000 spectrometer. Hydrogen nuclear magnetic resonance (^{1}H NMR) spectra were measured with a Varian Mercury Plus 400 MHz spectrometer. Thermal gravimetric analysis (TGA) was conducted on a PE TGA-7 instrument with a heating rate of 20 °C/min in a nitrogen flow (20 mL/min). Transmission electron microscopy (TEM) studies were performed on a JEOL JEM 2200FS field emission electron microscope (equipped with an energy-dispersive spectrometer, EDS) at 200 kV. Scanning electron microscopy (SEM) images were recorded using a LEO 1550VP field-emission microscope. The XRD patterns were recorded on a Rigaku X-ray diffractometer D/MAX-2200/pc equipped with Cu Kα radiation (40 kV, 20 mA) at a rate of 1.0°/min over the range of 20−70° (2θ). The experimental system for the manipulation is basically the same as the one shown in a previous paper.[17] A rotational magnetic field was produced using two pairs of coils, function generator (HP8904A, Agilent Technologies Inc.), and amplifiers (BOP-20-10M, KEPCO Inc.). The motion of the magnetic nanotubes and red blood cells was observed by a charge-coupled-device (CCD) high-speed camera system (VCC-H8000, Digimo Corp. Ltd.) with an object lens (VH-Z450, Keyence Corp.).

Grafting Poly(2-diethylaminoethyl methacrylate) onto MWNTs. MWNT-Br (100.0 mg), CuBr (16.8 mg, 0.120 mmol), PMDETA (20.8 mg, 0.120 mmol), and methanol (2 mL) were placed in a 10 mL dry flask. The flask was evacuated and filled thrice with Ar. Then 2-diethylaminoethyl methacrylate (DEAEMA, 500.0 mg) was injected into the flask, and the mixture was stirred at 60 °C for 48 h. The reaction mixture was diluted with tetrahydrofuran (THF) and thrice vacuum-filtered. The filtered solid was re-dispersed in THF, and then filtered and washed with THF four times. The sample of poly(2-diethylaminoethyl methacrylate)-grafted MWNTs (MWNT-*g*-PAm) was obtained after drying overnight under vacuum.

Assembling Iron Oxide Nanoparticles onto MWNTs. Typically, MWNT-*g*-PAm (82 mg), deionized water (40 mL), and methyl iodide (2 mL) were placed in a 100 mL flask. The mixture was sonicated for 5 min and then stirred at room temperature for 94 h. The resulting sample was separated by repeated centrifugation. The as-quaternized MWNT-*g*-PAm (25 mg) and deionized water (100 mL) were placed in a 500 mL flask and sonicated for 5 min. Subsequently, the diluted magnetic fluid W-40 (150 mL, ca. 0.15 mL of the original solution) was added dropwise into the flask under stirring. The mixture was stirred at room temperature for 15 h. The resulting product was collected by repeated centrifuging followed by vacuum drying. EDS measurements showed that the sample contains ca. 22.5 wt % of elemental iron.

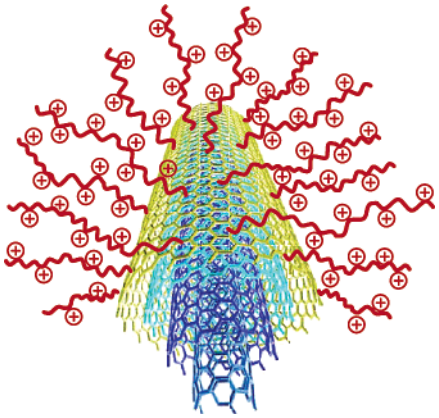

Figure 1. Cartoon of a cationic multiarm MWNT-based nanocatcher.

Magnetic Manipulation of Blood Cells. The magnetic carbon nanotubes were placed into a phosphate-buffered saline (PBS) solution (pH 7.4) and dispersed using a sonicator. Sheep's erythrocytes were also dispersed in a different PBS solution, to which the nanotube solution was added. The erythrocytes−magnetic nanotubes mixture was shaken gently for 10 min, dropped onto a slide glass, and covered with a thin glass plate for observation. The sample was placed in a rotational magnetic field produced by coils, function generator, and amplifiers. The dynamics of erythrocytes, to which the magnetic nanotubes are attached, was observed using a CCD high-speed camera and recorded on the hard disk of a computer.

3. Results and Discussion

3.1. Design of Synthesis Strategy. Our strategy to synthesize the magnetic CNTs contains two main steps: (1) covalent grafting of cationic polymer chains onto MWNT surfaces to prepare nanocatchers (a cartoon of a nanocatcher, a MWNT immobilized with multiple cationic polymer arms, is shown in Figure 1), and (2) assembling magnetic nanoparticles onto the polyelectrolyte-coated MWNTs (so-called nanocatchers). Evidently, the functionalized CNTs possess numerous polyelectrolyte arms, resembling octopuses, which can easily catch and strongly hold its quarries with opposite charges by the strong electrostatic attraction. The specific synthesis procedures are depicted in Scheme 1. First, the oxidized MWNTs (MWNT-COOH) were reacted with excess thionyl chloride and glycol, generating hydroxyl-functionalized MWNTs (MWNT-OH). MWNT-OH was reacted subsequently with 2-bromo-2-methylpropionyl bromide to provide MWNT-based macroinitiator, MWNT-Br.[16] By in situ atom transfer radical polymerization (ATRP) of 2-diethylaminoethyl methacrylate (DEAEMA)[18,19] initiated with MWNT-Br, poly(2-diethylaminoethyl methacrylate) (PEMAEMA) was covalently grafted onto MWNTs.[20] Then, the polyamine-grafted MWNTs (MWNT-*g*-PAm) were quaternized with methyl iodide, affording cationic polyelectrolyte-grafted MWNTs (MWNT-*g*-PAmI). Finally, anionic magnetic iron oxide (Fe_3O_4) nanoparticles were facilely loaded onto the MWNT surfaces by electrostatic assembling between MWNT-PAmI and Fe_3O_4, giving rise to magnetic nanotubes or nanohybrids. This approach is provided with at least four virtues. (1) General: both materials of CNTs and iron oxide are commercially available; the supported raw material can be SWNTs, MWNTs, carbon fibers, and even carbon spheres,

SCHEME 1

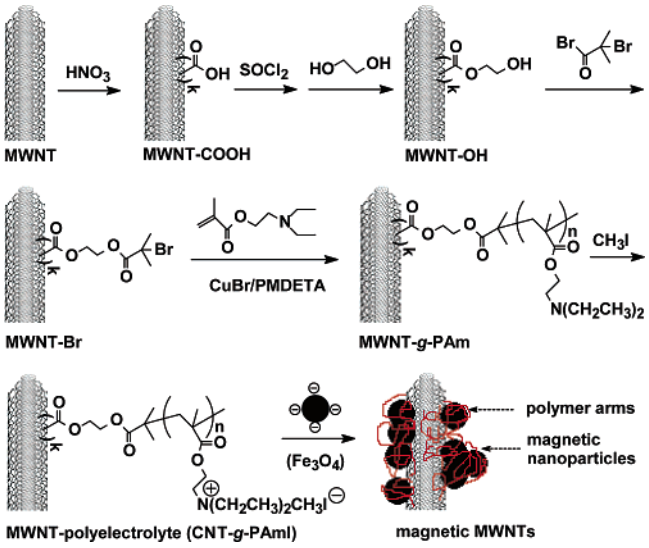

which are made by CVD or any other techniques, and the grafted polyelectrolyte can be either cationic or anionic polymer, and the assembled functional compounds can be any of magnetic, optical, luminescent, radio absorbable, and other kinds of nanoparticles. (2) Controllable: the grafted polymer quantity and electrostatic force (or pH value of solution) are controllable, resulting in high controllability of the content of loaded nanoparticles. (3) Stable: the loaded nanoparticles are very stable on the tube surfaces because of the strong interactions among CNT, polymer arms, and nanoparticles. (4) Highly loadable: the loading capability is quite high because of the high area of nanotubes and strong electrostatic force.

3.2. Characterization of Polyamine-Grafted MWNTs. The grafted polyamine (PDEAEMA) content, determined by TGA measurement, was 60 wt %. The chemical structure of the MWNT-*g*-PAm was confirmed with FTIR and NMR measurements (see Supporting Information, SM 1). The characteristic absorption peaks of PDEAEMA, such as −C═O− and −C−H− stretching vibrations, appeared clearly at 1724 and 2800−3000 cm^{-1} in the FTIR spectrum of MWNT-*g*-PAm. In the ^1H NMR spectrum of MWNT-*g*-PAm, the proton signals of $-CH_2O-$, $-OCH_2CH_2N-$, CH_3CH_2N-, $-CH_2C-$, CH_3CH_2N-, and CH_3C- groups were found as peaks at δ 4.05, 2.75, 2.6, 1.9, 1.05, and 0.85 ppm, respectively.

The nanostructures and morphology of the resulting MWNT-*g*-PAm hybrids were observed with HRTEM and SEM. The surface of the pristine MWNT without functionalization is featureless, and there are little or no traces of amorphous carbon (Figure 2a). After grafting PDEAEMA onto the tube surface, a core−shell structure was formed. The tube was enwrapped by several nanometers (ca. 3−5 nm) of polymer chains under the HRTEM observation (Figure 2b). It is noteworthy that the TEM electron beam at high resolution may destroy the grafted polymer chains, resulting in a probably lower limit of the polymer shell thickness that appears in the image. The morphology of mass tubes was perceived by SEM measurements. The pristine nanotubes are very smooth and separated from each other (Figure 2c), while the polyamine-grafted tubes exhibit a distinctive morphology: many tubes nestle closely or even cuddle each other because of the coverage of polymer chains and the interaction among the chains (Figure 2d). All of the analyses described above confirmed that PDEAEMA was successfully grafted onto the nanotube convex surfaces, forming the precursor of the multiarm nanocatcher.

3.3. Synthesis and Characterization of Magnetic Carbon Nanotubes. The polyamine-grafted nanotubes can be directly used to catch anionic compounds by adjusting the pH of the solution, and they can be modified in advance with alkyl halide to produce polycations and then catch quarries without pH adjusting as well. We tried both routes and succeeded in attaching iron oxide nanoparticles onto the nanotubes. Herein,

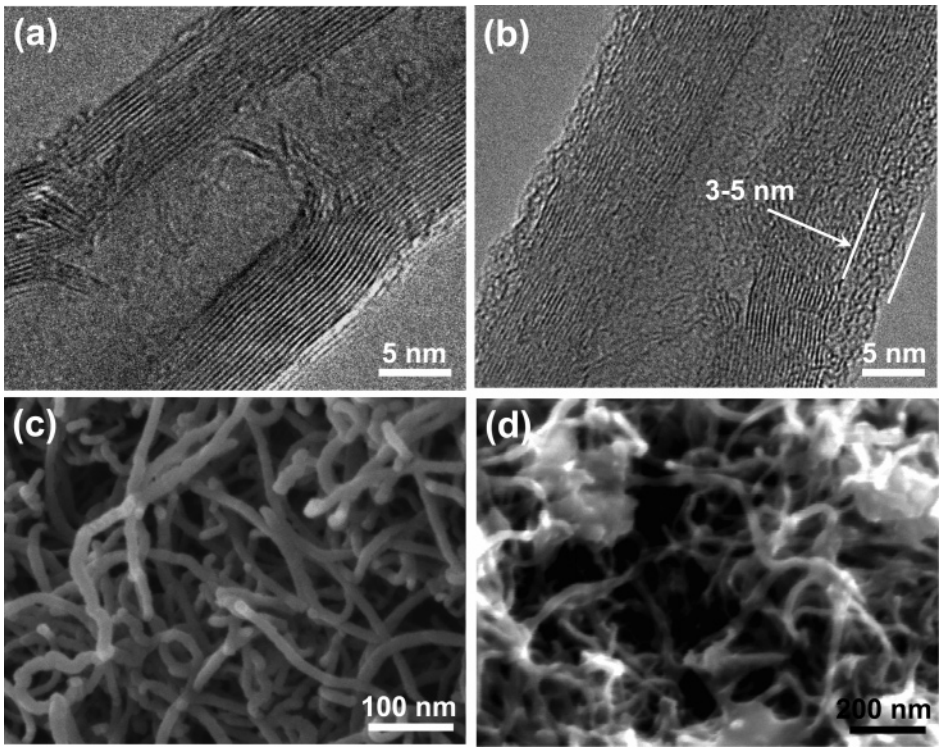

Figure 2. Representative HRTEM images of pristine MWNT (a) and MWNT-*g*-PAm (b), and SEM images of pristine MWNTs (c) and MWNT-*g*-PAm (d).

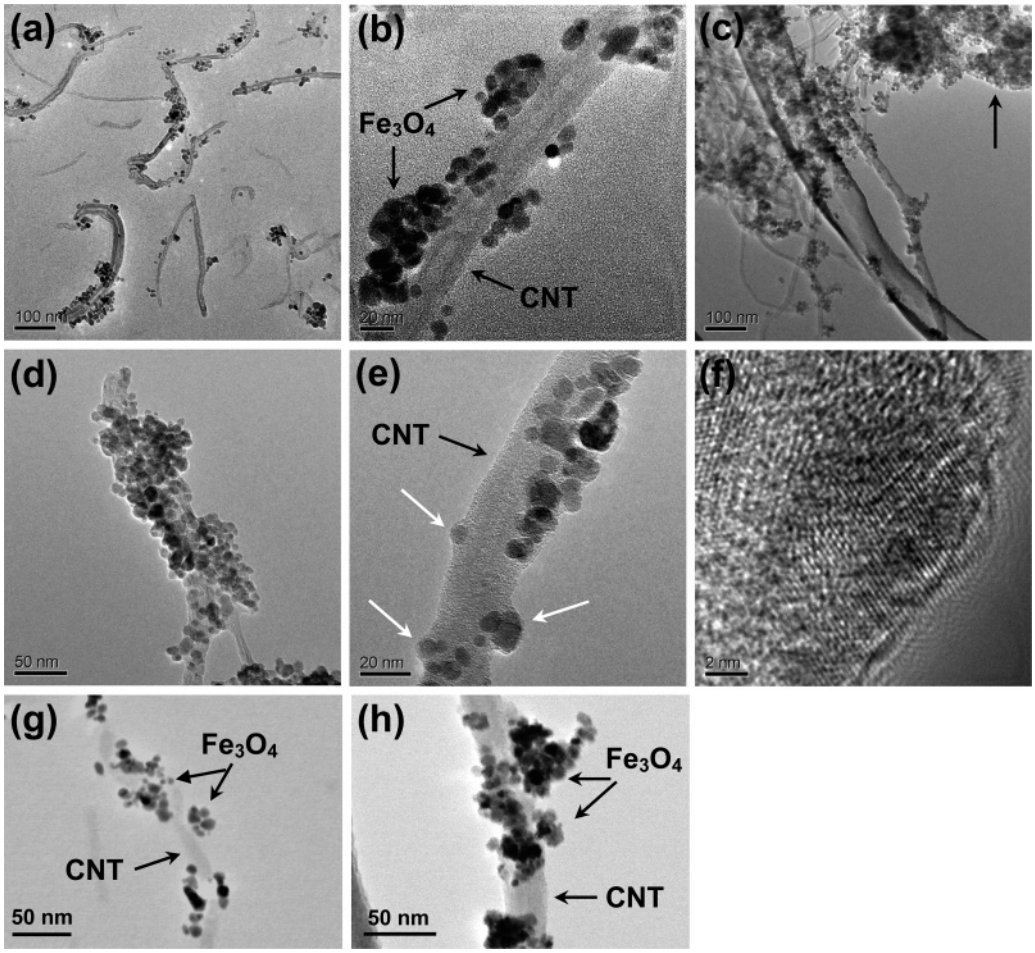

Figure 3. Representative TEM images of the magnetic nanotube sample with 6.3 wt % of iron (a, b) and the sample with 22.5 wt % of iron (c−e). HRTEM image of an iron oxide nanoparticle attached on tube surface, showing the lattice of iron oxide crystal (f). STEM images of the magnetic nanotube samples with 6.3 (g) and 22.5 (h) wt % of iron. The scale bars in a, b, c, d, e, and f correspond to 100, 20, 100, 50, 20, and 2 nm, respectively.

we report the loading results of methyl iodide-modified MWNT-*g*-PAm (MWNT-*g*-PAmI). In the magnetic particles' attachment process to carbon nanotubes we used a magnetic fluid W-40 produced by Taiho Co. Ltd. It is a water-based colloidal solution in which Fe_3O_4 magnetic nanoparticles ca. 10 nm in diameter are dispersed. The loaded nanoparticle content can be adjusted by changing the feed ratio of Fe_3O_4 to MWNT-*g*-PAmI (nanocatcher). When the loaded amount was low (<ca. 8 wt % of iron), no mass precipitation appeared during the synthesis and the resulting magnetic nanotubes could be relatively well dispersed in water. When the loaded amount was high (>ca. 25 wt % of iron), the nanotubes assembled rapidly and precipitated soon from the solution in the experiment and the obtained magnetic object could not be well re-dispersed in water after drying. The crystalline structure of the resulting magnetic nanotubes was confirmed with powder XRD measurements, and the main peaks of Fe_3O_4 crystals were clearly presented (see Supporting Information, SM2).

Figure 3 displays the TEM images of magnetic nanotube samples containing ca. 6.3 and 22.5 wt % of elemental iron (the iron content was determined by EDS with 3−4 areas of each TEM sample). For the sample containing a lower amount of iron oxide (Figure 3a), the tubes were well dispersed in the solution and thus individually lay down on the TEM grid. Most of tubes were loaded with iron oxide nanoparticles. No separated nanoparticles were found on the TEM carbon film, which suggests that the unattached nanoparticles have been completely removed from the product. At a higher magnification nanotube and its loaded nanoparticles can be clearly observed, and some nanoparticles assembled into nanoclusters but still adhered stably on the tube surface (Figure 3b). For the sample with higher content of iron oxide, magnetic nanohybrids and even nanocomposites were observed in which the iron oxide concentration is too high to observe nanotubes distinctly for some crossed tube nets (Figure 3c, marked area by an arrow). For some separately tubes the nanoclusters organized with the iron oxide nanoparticles can completely enwrap the tubes, affording core−shell magnetic nanostructures (Figure 3d). To ascertain the attaching status of the nanoparticles on the tube surface we carefully selected a magnetic tube possessing individual nanoparticles whose attached side can be clearly observed. The nanoparticles attached on the tube surface so tightly and perfectly that they look like nodes growing from the tube, as marked by the white arrows in Figure 3e. Such strong and complete attachment can be attributed to the cationic multiple arms grown on the tubes. Furthermore, each arm consists of 20−60 amino units. Thus, an anionic nanoparticle can be attracted and then entangled, held, or adhered by the cationic multifigure arms via polytopic electrostatic, van der Waals, and mechanical forces. The HRTEM measurement indicated that the attached nanoparticles are still crystalline since the crystal lattice was clearly observed (Figure 3f). To confirm the structure of the magnetic tubes, we conducted scanning transmission electron microscopy (STEM) studies, which may provide morphological images with high contrast of different matters because of different electron transmission ability. As shown in

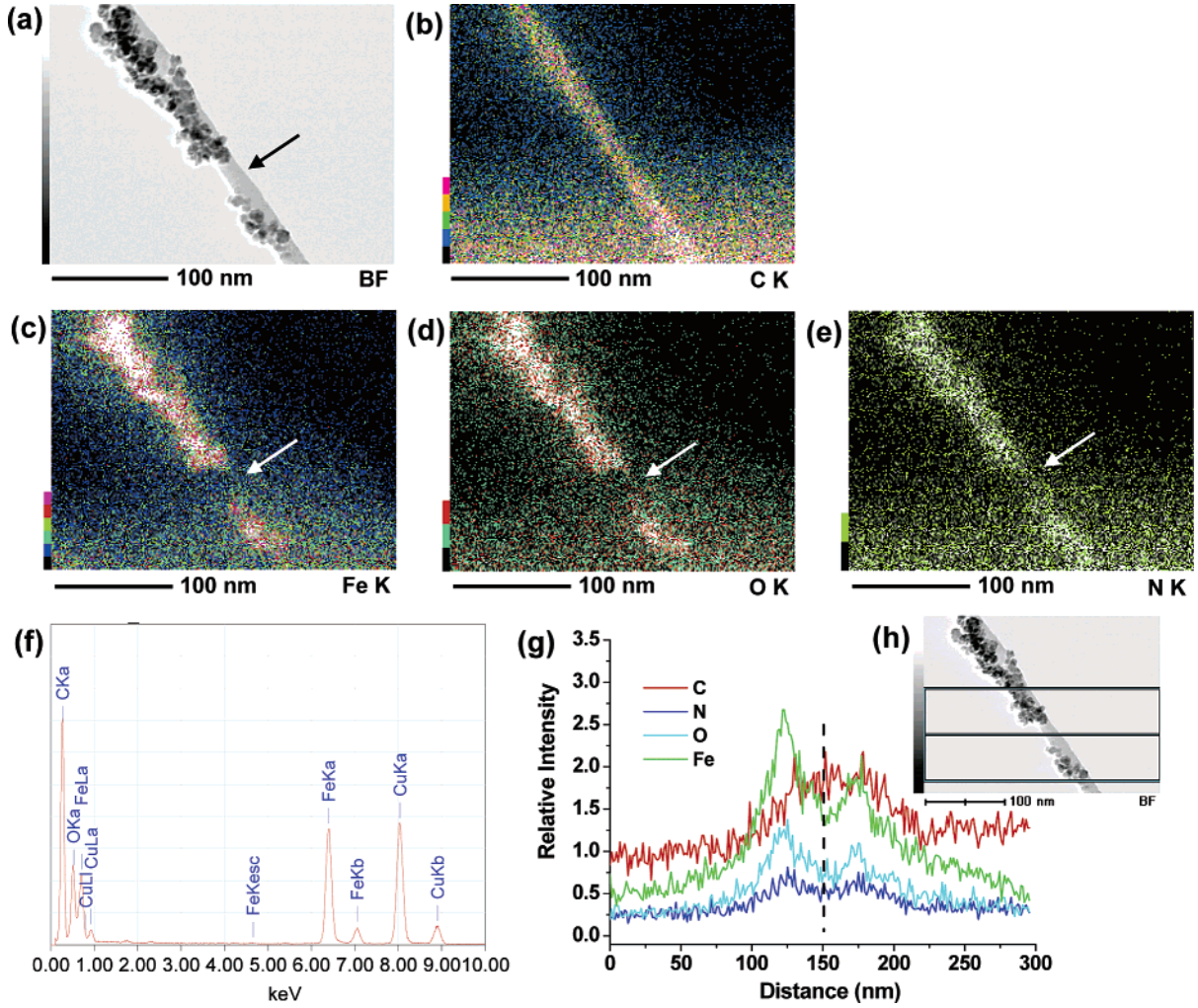

Figure 4. Elemental mapping and EDS of a magnetic nanotube of the sample with 22.5 wt % of iron: (a) bright field image; (b, c, d, and e) carbon, iron, oxygen, and nitrogen maps; (f) EDS of the magnetic tube; (g and h) elemental linear profiles of the magnetic tube and corresponding analyzed tube area.

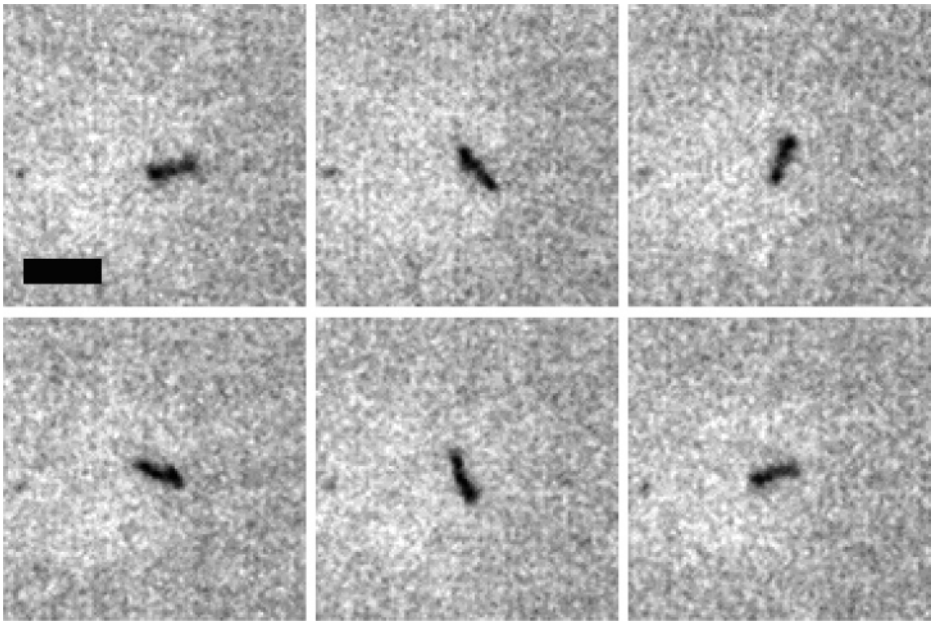

Figure 5. Rotational motion of a bundle of magnetic nanotubes in a rotational magnetic field. The frequency and intensity of the magnetic field are 0.5 Hz and 12.7 kA/m. The bundle of the magnetic nanotubes is rotated in the clockwise direction. The snapshots correspond to 0th, 0.2th, 0.4th, 0.6th, 0.8th, and 1.0th cycle of the rotational magnetic field. The scale bar is 5 μm.

Figure 3g and h the black particles are iron oxide and the rodlike gray structure is the nanotube.

The components and their distributions of the resulting magnetic nanotubes were assayed by energy-dispersive spectrum

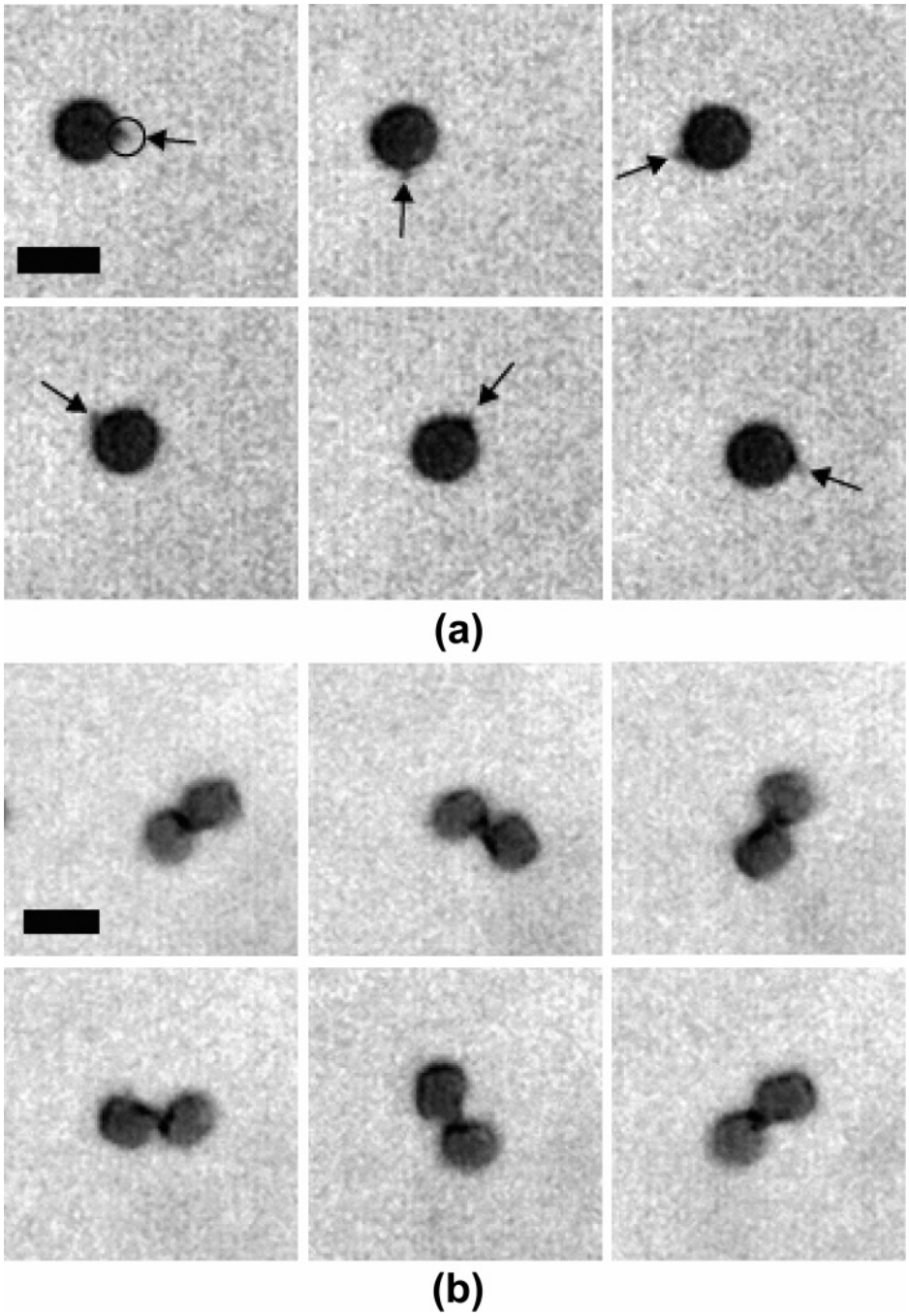

Figure 6. Rotational motion of sheep red blood cells. Magnetic nanotubes are attached to the cells. The frequency and intensity of the magnetic field are 0.5 Hz and 12.7 kA/m. The snapshots correspond to 0th, 0.2th, 0.4th, 0.6th, 0.8th, and 1.0th cycle of the rotational magnetic field. The blood cells are rotated in the clockwise direction. The scale bars are 5 μm. (a) A sheep red blood cell. Magnetic nanotubes indicated by an arrow are attached to the cell. (b) Two sheep red blood cells bridged with magnetic nanotubes.

(EDS) and elemental mapping analyses. Figure 4 shows the elemental mapping and EDS results of a section of a selected magnetic tube. On this tube there is a short segment covered without iron oxide, which looks like a nick of the magnetic tube (see Figure 4a, the nick is designated by an arrow). The carbon map is continuous and relatively symmetric and smooth, matching with the bright field (BF) image very well (Figure 4b). The maps of iron and oxygen also match the silhouette of black nanoparticles shown in Figure 4a very well in both distribution and concentration. Significantly, the nick segment of the magnetic tube also corresponds fully with the discontinuous gap of iron and oxygen profiles (Figure 4c and d, the gap is denoted with an arrow). These analyses further demonstrate that the black particles are iron oxide, and the nanoparticles were successfully assembled onto the tube surface with a high concentration. Interestingly, the nitrogen profile likely discloses the reasons of the nick appearance and the strong attaching as only the grafted polymer chains contain nitrogen element (see Figure 4e). Evidently, the mapping profile of nitrogen is in fine accordance with those of iron and oxygen, while it is distinct from that of carbon. A discontinuous gap in the nitrogen map is also found at the identical area of the magnetic tube (Figure 4e, marked by an arrow). This result clarifies that (1) the bald area of magnetic tubes resulted from rare or no polymer arms grown there, (2) the higher the concentration of nitrogen element or polymer grafts the greater the content of loaded iron oxide nanoparticles, and (3) the strong and high loading is ascribed to the tethered ionic polymer arms and their concomitant

functions. In the EDS spectrum of this tube iron signal is also very strong and the weight content of iron is as high as 20.3 wt % (Figure 4f). Figure 4g displays the line profile analyzing spectrum of the selected area which is demarcated with two blue rectangles in Figure 4h. A saddle-like spectrum with a valley at a distance of 150 nm is observed for iron, oxygen, and nitrogen. In the carbon spectrum, on the contrary, only one big protuberant peak is found and no valley appears at a distance of 150 nm. All of these spectra are in agreement with element distributions of the demarcated tube, which has a bald area at a distance of 150 nm.

3.4. Application of Magnetic Nanotubes in Biomanipulations. Magnetic property measurement demonstrated that the obtained magnetic tubes are paramagnetic (same as the iron oxide nanoparticles), and the higher the concentration of loaded nanoparticles, the greater the magnetic density (data not shown). Therefore, the magnetic nanotubes have tremendous potential in applications of magnetic materials and functional nanomaterials and nanodevices if considering their general and facile fabrications. As an example of an application, we used the magnetic tubes as the magnetic handle to manipulate blood cells in a magnetic field. Magnetic biomanipulations such as cell, gene, and DNA manipulations play significant roles in bioengineering, biomedical therapy, and single-object technology. Magnetic beads have been actively used recently in cell biology research such as cell separations and the manipulations of cells and cell membranes.[21−25] Hultgren et al. examined the performance of the cell separations by Ni nanowires and concluded that nanowires, in general, are superior to magnetic beads in both purity and yield of the separated cells due to the larger surface area,[22] which suggests that carbon nanotubes may also perform efficiently in the cell biology field. However, magnetic carbon nanotubes have not yet been used for the separations and manipulations of cells. Here, we demonstrate the manipulation of sheep red blood cells using our magnetic carbon nanotubes.

Since the volume of the blood cell is very big (ca. 4 μm in diameter), it needs a relatively strong magnetic force to manipulate cells in a buffer solution. The nanotubes loaded with a higher amount of iron oxide are probably able to perform it. First, the magnetic nanotubes themselves were manipulated in the buffer solution under the magnetic field to test the magnetic activity of the tubes. The process was recorded by an optical microscope equipped with a high-speed camera. Owing to the magnification limitation of the optical microscope, the individual nanotubes cannot be perceived, so only the performances of bundles assembled with nanotubes were photographed. The magnetic bundles can be easily rotated in the solution, and the rotation speed can be effectively controlled by changing the frequency of the magnetic field. No decrease of magnetic activity was found after keeping the tubes in the buffer solution for 2 days. One cut of the snapshots is exhibited in Figure 5. These tests implied that the magnetic tubes are quite robust and stable.

The magnetic nanotubes were then employed to manipulate the sheep blood cells. In a two-dimensional (2D) rotation magnetic field, those blood cells attached with magnetic nanotubes can be rotated at a rapid speed. The magnetized blood cells can also be aligned or conveyed from one site to another site by changing the magnetic field directions. Blood cells without nanotubes cannot be rotated or controllably conveyed. A typical example of rotation manipulation for one blood cell is displayed in Figure 6a as cut photographs. This blood cell was clockwise rotated with a speed of 1 cycle per 3 s under the 0.5 Hz and 12.7 kA/m magnetic field. Because of the bridging of magnetic nanotubes, two blood cells can be manipulated together, as shown in Figure 6b. The two cells were rotated with a speed of one cycle per ca. 3 s under the same magnetic field. Such selective biomanipulations open a door to manage and operate individual bioobjects and build novel artificial biostructures by a magnetic handle.

4. Conclusions

A facile approach to magnetic nanotubes was presented. Cationic multiarm nanocatchers were prepared by the grafting from approach in the presence of MWNT-based macroinitiator, MWNT-Br. Depending on the strong electrostatic attraction between opposite charges and other interactions, the paramagnetic iron oxide nanoparticles were assembled onto the convex surfaces of nanocatchers, affording paramagnetic nanotubes. This approach possesses the advantages of generality, reproducibility, controllability, tailor ability, high-loading capability, and stability, promising wide applications of the resulting magnetic and other functional nanohybrids. The grafted polymer chains can be extended to anionic macromolecules such as poly(acrylic acid) and poly(sodium 4-stryrenesulfonate) to produce anionic nanocatchers, which can be used to load metal ions and cationic matters, offering novel nanomaterials and nanodevices. The magnetic nanotubes can be easily manipulated in the magnetic field. Thus, they were used as the magnetic handle to manipulate sheep red blood cells. Blood cells in a buffer solution can be selectively rotated or conveyed in a magnetic field, which shows applications of magnetic nanotubes in the field of bioengineering, single-object technology, and biomedical therapy.

Acknowledgment. This work was financially supported by the National Natural Science Foundation of China (Nos. 50473010 and 20304007), Fok Ying Tung Education Foundation (No. 91013), Rising-Star Program Foundation of Shanghai (No. 03QB14028), EPSRC, and 21st Century's Centre of Excellence Program of Japan. We thank Prof. Sir Harold W. Kroto (The Florida State University) and Dr. Raymond L. D. Whitby (University of Sussex, U.K.) for helpful contributions. We are also grateful to Mr. Keiichi Hirakawa (Toyo University, Japan) for technical assistance with HRTEM and EDS.

Supporting Information Available: FTIR and ^{1}H NMR spectra of MWNT-*g*-Pam (SM1), and XRD patterns of Fe_3O_4-loaded magnetic MWNTs and neat Fe_3O_4 nanoparticles (SM2). This material is available free of charge via the Internet at http://pubs.acs.org.

References and Notes

(1) Iijima, S. *Nature* **1991**, *354*, 56−58.

(2) (a) Dai, L.; Mau, A. W. H. *Adv. Mater.* **2001**, *13*, 899−913. (b) Niyogi, S.; Hamon, M. A.; Hu, H.; Zhao, B.; Bhowmik, P.; Sen, R.; Itkis, M. E.; Haddon, R. C. *Acc. Chem. Res.* **2002**, *35*, 1105−1113.

(3) Gao, Y. H.; Bando, Y. *Nature* **2002**, *415*, 599−599.

(4) Hernandez, E.; Meunier, V.; Smith, B. W.; Rurali, R.; Terrones, H.; Nardelli, M. B.; Terrones, M.; Luzzi, D. E.; Charlier, J. C. *Nano Lett.* **2003**, *3*, 1037−1042.

(5) Regan, B. C.; Aloni, S.; Ritchie, R. O.; Dahmen, U.; Zettl, A. *Nature* **2004**, *428*, 924−927.

(6) (a) Lin, Y.; Taylor, S.; Li, H.; Fernando, S.; Qu, L.; Wang, W.; Gu, L.; Zhou, B.; Sun, Y.-P. *J. Mater. Chem.* **2004**, *14*, 527−541. (b) Sun, Y.-P.; Fu, K.; Lin, Y.; Huang, W. *Acc. Chem. Res.* **2002**, *35*, 1096−1104.

(7) (a) Chen, R. J.; Zhang, Y.; Wang, D.; Dai, H. J. *J. Am. Chem. Soc.* **2001**, *123*, 3838−3839. (b) Azamian, B.; Davis, J.; Coleman, K.; Bagshaw, C.; Green, M. L. H. *J. Am. Chem. Soc.* **2002**, *124*, 12664−12665. (c) Georgakilas, V.; Tzitzios, V.; Gournis, D.; Petridis, D. *Chem. Mater.* **2005**, *17*, 1613−1617.

(8) (a) Banerjee, S.; Wong, S. S. *Nano Lett.* **2002**, *2*, 49−53. (b) Banerjee, S.; Wong, S. S. *J. Am. Chem. Soc.* **2002**, *124*, 8940−8948. (b) Frehill, F.; Vos, J. G.; Benrezzak, S.; Koós, A. A.; Kónya, Z.; Rüther, M. G.; Blau, W. J.; Fonseca, A.; Nagy, J. B.; Biró, L. P.; Minett, A. I.; Panhuis, M. I. H. *J. Am. Chem. Soc.* **2002**, *124*, 13694−13695.

(9) Richard, C.; Balavoine, F.; Schultz, P.; Ebbesen, T. W.; Mioskowski, C. *Science* **2003**, *300*, 775−778.

(10) For example, see: (a) Kong, H.; Gao, C.; Yan, D. *J. Am. Chem. Soc.* **2004**, *126*, 412−413. (b) Yao, Z.; Braidy, N.; Botton, G. A.; Adronov, A. *J. Am. Chem. Soc.* **2003**, *125*, 16015−16024. (c) Qin, S.; Qin, D.; Ford, W. T.; Resasco, D. E.; Herrera, J. E. *J. Am. Chem. Soc.*, **2004**, *126*, 170−176. (d) Qin, S. H.; Qin, D. Q.; Ford, W. T.; Herrera, J. E.; Resasco, D. E.; Bachilo, S. M.; Weisman, R. B. *Macromolecules* **2004**, *37*, 3965−3967. (e) Koshio, A.; Yudasaka, M.; Zhang, M.; Iijima, S. *Nano Lett.* **2001**, *1*, 361−363. (f) Riggs, J. E.; Guo, Z.; Carroll, D. L.; Sun, Y.-P. *J. Am. Chem. Soc.* **2000**, *122*, 5879−5880. (g) Baskaran, D.; Mays, J. W.; Bratcher M. S. *Angew. Chem., Int. Ed.* **2004**, *43*, 2138−2142. (h) Zhao, B.; Hu, H.; Haddon, H. C. *Adv. Funct. Mater.* **2004**, *14*, 71−76. (i) Kahn, M. G. C.; Banerjee, S.; Wong, S. S. *Nano Lett.* **2002**, *2*, 1215−1218. (j) Huang, W.; Fernando, S.; Allard, L. F.; Sun, Y.-P. *Nano Lett.* **2003**, *3*, 565−568. (k) Fu, K.; Huang, W.; Lin, Y.; Riddle, L. A.; Carroll, D. L.; Sun, Y.-P. *Nano Lett.* **2001**, *1*, 439−441.

(11) (a) Li, J.; Moskovits, M.; Haslett, T. L. *Chem. Mater.* **1998**, *10*, 1963−1967. (b) Choi, H. C.; Shim, M.; Bangsaruntip, S.; Dai, H. *J. Am. Chem. Soc.* **2002**, *124*, 9058−9059. (c) Xing, Y. C. *J. Phys. Chem. B* **2004**, *108*, 19255−19259. (d) Kim, B.; Sigmund, W. M. *Langmuir* **2004**, *20*, 8239−8242. (e) Qu, L. T.; Dai, L. M. *J. Am. Chem. Soc.* **2005**, *127*, 10806−10807. (f) Zhan, J. H.; Bando, Y.; Hu, J. Q.; Liu, Z. W.; Yin, L. W.; Golberg, D. *Angew. Chem., Int. Ed.* **2005**, *44*, 2140−2144.

(12) Lee, S. W.; Sigmund, W. M. *Chem. Commun.* **2003**, 780−781.

(13) (a) Huang, Q.; Gao, L. *Nanotechnology* **2004**, 1855−1860. (b) Shi, J. H.; Qin, Y. J.; Wu, W.; Li, X. L.; Guo, Z.-L.; Zhu, D. B. *Carbon* **2004**, *42*, 423−426. (c) Cao, J.; Sun, J.-Z.; Hong, J.; Li, H.-Y.; Chen, H.-Z.; Wang, M. *Adv. Mater.* **2004**, *16*, 84−87. (d) Banerjee, S.; Wong, S. S. *J. Am. Chem.* Soc. **2003**, *125*, 10342−10350. (e) Banerjee, S.; Wong, S. S. *Chem. Commun.* **2004**, 1866−1867.

(14) Korneva, G.; Ye, H.; Gogotsi, Y.; Halverson, D.; Friedman, G.; Bradley, J.-C.; Kornev, K. G. *Nano Lett.* **2005**, *5*, 879−884.

(15) Georgakilas, V.; Tzitzios, V.; Gournis, D.; Petridis, D. *Chem. Mater.* **2005**, *17*, 1613−1617.

(16) Kong, H.; Gao, C.; Yan, D. *Macromolecules* **2004**, *37*, 4022−4030.

(17) Nagaoka, Y.; Morimoto, H.; Maekawa, T. *Phys. Rev. E* **2005**, *71*, Art. No. 032502.

(18) (a) Pyun, J.; Kowalewski, T.; Matyjaszewski, K. *Macromol. Rapid Commun.* **2003**, *24*, 1043−1059. (b) Coessens, V.; Pintauer, T.; Matyjaszewski, K. *Prog. Polym. Sci.* **2001**, *26*, 337−377. (c) Pyun, J.; Matyjaszewski, K. *Chem. Mater.* **2001**, *13*, 3436−3448. (d) Matyjaszewski, K.; Xia, J. H. *Chem.* Rev. **2001**, *101*, 2921−2990. (e) Wang, J. S.; Matyjaszewski, K. *J. Am. Chem. Soc.* **1995**, *117*, 5614−5615. (f) Kato, M.; Kamigaito, M.; Sawamoto, M.; Higashimura, T. *Macromolecules* **1995**, *28*, 1721−1723.

(19) (a) Webber, G. B.; Wanless, E. J.; Butun, V.; Armes, S. P.; Biggs, S. *Nano Lett.* **2002**, *2*, 1307−1313. (b) Gan, L. H.; Ravi, P.; Mao, B.; Tam, K. C. *J. Polym. Sci., Part A: Polym. Chem.* **2003**, *41*, 2688−2695. (c) Amalvy, J. I.; Wanless, E. J.; Li, Y.; Michailidou, V.; Armes, S. P.; Duccini, Y. *Langmuir* **2004**, *20*, 8992−8999. (d) Bütün, V. *Polymer* **2003**, *44*, 7321−7334. (e) Liu, S.; Weaver, J. V. M.; Save, M.; Armes, S. P. *Langmuir* **2002**, *18*, 8350−8357.

(20) (a) Li, W. W.; Kong, H.; Gao, C.; Yan, D. Y. *Chin. Sci. Bull.* **2005**, *50*, 2276−2280. (b) Gao, C.; Vo, C. D.; Jin, Y. Z.; Li, W. W.; Armes, S. P. *Macromolecules* **2005**, *38*, 8634−8648.

(21) Fabry, B.; Maksym, G. N.; Butler, J. P.; Glogauer, M.; Navajas D.; Fredberg, J. J. *Phys. Rev. Lett.* **2001**, *87*, 148102.

(22) Hultgren, A.; Tanase, M.; Chen, C. S.; Meyer, G. J.; Reich, D. H. *J. Appl. Phys.* **2003**, *93*, 7554−7556.

(23) Hosu, B. G.; Jakab, K.; Bánki, P.; Tóth, F. I.; Forgacs, G. *Rev. Sci. Instrum.* **2003**, *74*, 4158−4163.

(24) Berry, C. C.; Curtis, A. S. G. *J. Phys. D: Appl. Phys.* **2003**, *36*, R198−R206.

(25) (a) Lee, H.; Purdon A. M.; Westervelt, R. M. *Appl. Phys. Lett.* **2004**, *85*, 1063−1065. (b) Lee, H.; Purdon, A. M.; Chu, V.; Westervelt, R. M. *Nano Lett.* **2004**, *4*, 995−998.